CHANNEL CORRELATION AND POWER CONTROL IN MEO CONSTELLATIONS

Olivier Grémillet[(1)] **, Axel Jahn**[(1)]**, Richard Wyrwas**[(2)]
[(1)]***DLR – German Aerospace Center***
Oberpfaffenhofen, Germany
{Olivier.Gremillet, Axel.Jahn}@dlr.de

[(2)] ***ICO Global Communications,***
Symphony House, Cowley Business Park, Uxbridge, Middlesex, UB8 2AD, England,
Richard.Wyrwas@ico.com

ABSTRACT

In this paper a MEO channel measurement campaign with focus on correlation between forward and backward channels is presented. The results for different scenarios are analysed. The effect of the channel correlation on power control is studied using the measured propagation data.

INTRODUCTION

Propagation experiments are fundamental for the design of satellite systems [1]. Especially in constellations with non-geostationary orbits, such as the ICO system [2] propagation impairments must be compensated by appropriate countermeasures such as link margins, power control and satellite diversity. DLR and ICO Global Communications have conducted a measurement campaign to determine the propagation effects on the satellite uplink and downlink using several satellite diversity paths and to analyse the channel correlation and its effects on different power control schemes. S-Band transmission frequencies just above the UMTS band were used in these trials.

In the first part of this paper the measurement campaign is presented. The large number of gathered propagation data enabled the behaviour prediction of the future system for a wide range of environmental and users conditions. The main results of this campaign are presented in the second part of the paper.

MEASUREMENT CAMPAIGN

The measurement campaign used a Zeppelin airship to emulate different satellite orbit characteristics, cf. Fig. 1. A second transmitter/receiver was placed on top of high buildings for diversity reception. A user terminal was built to transmit and receive a CW signal in different frequency bands simultaneously. The frequency bands used were: 1986 MHz for the subscriber up-link, 2200 MHz and 2195 MHz for the subscriber down-link. The received signal was recorded in inphase and quadrature component on a digital DAT recorder. Additionally, the positions and the attitude of the user and Zeppelin were recorded on laptop computers. Also, video footage of the user operation was recorded during all tests. The dynamic range of the overall measurement set-up was better than 45 dB at nominal conditions. Various trials have been performed in June 1999 in the Bodensee area near Lindau and Friedrichshafen, Germany. The trials reflect several operational scenarios and environments. The environments comprise open, rural (various degrees of shadowing), suburban, urban, indoor hotel, indoor residential, indoor office, lakeside and ferry environments. Operational scenarios are typically handheld scenes, but also in-car scenarios, and scenarios where the handset was placed in pockets, briefcases, on tables, bedside tables and so forth.

THEORETICAL PROPAGATION MODEL

Several models for land mobile communications have been developed using measured data. The measurements collected during this campaign can be applied to communication systems where moving satellite are used. Those results have indicated that a significant proportion of the total energy typically arrives at the receiver from a direct wave. The remainder of the power is received via a ground-reflected wave and many randomly scattered rays which form a diffuse signal.

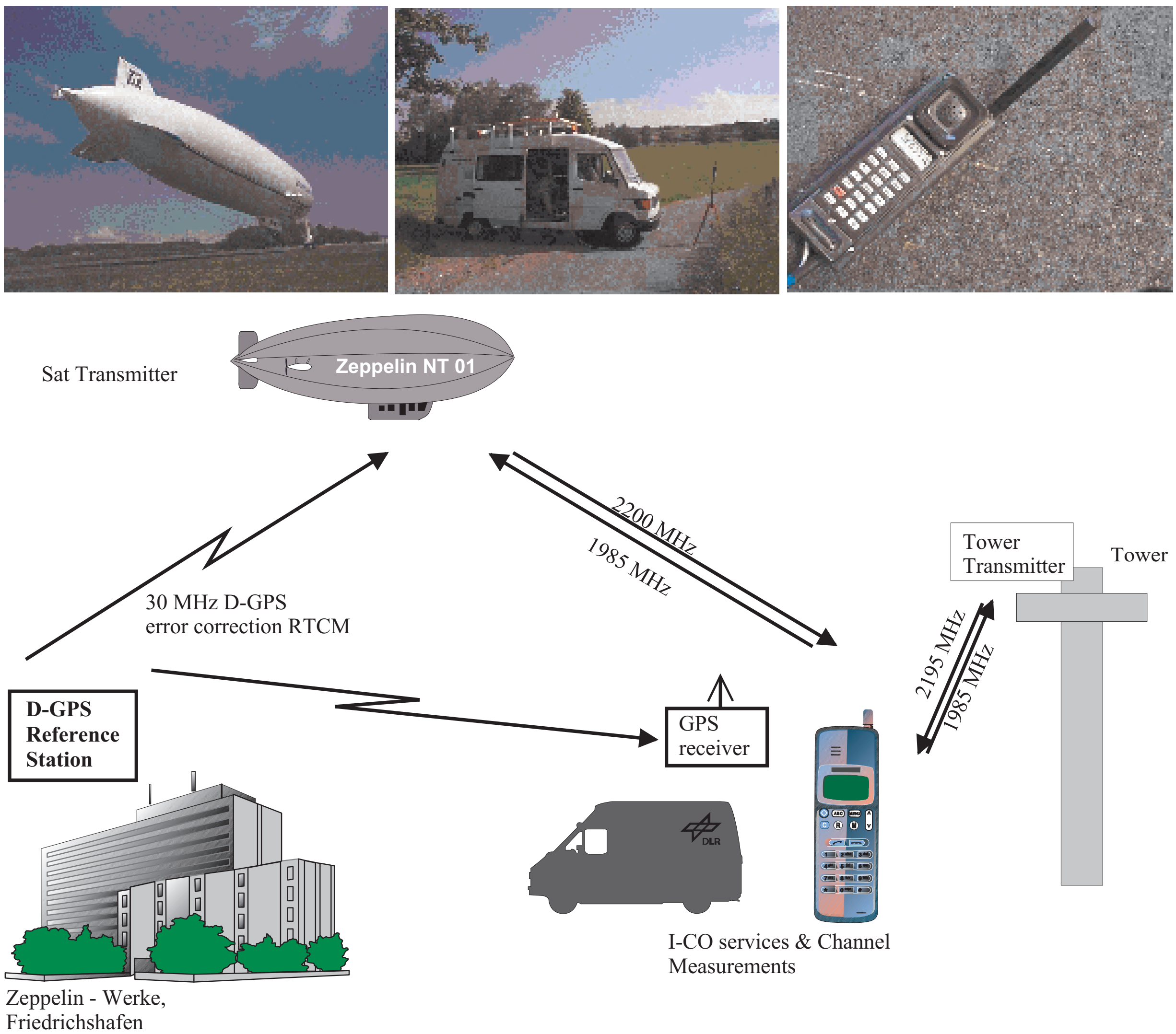

Figure 1: Measurement set-up

The received signal $r(t)$ is modelled by 3 components : $a(t)$, the direct signal component, $s(t)$ the specular reflection component reflected for smooth surfaces close to the user and $d(t)$ the diffuse component so that $r(t) = a(t)+s(t)+d(t)$. This model expands the Lutz model [3] and is called "propagation channel with single specular reflection". In this model the different components are:

$$a(t) = a_0.e^{j(w_c.t+\Phi)}$$
$$s(t) = s_0.e^{j(w_c.t+\Phi^{'})}$$
$$d(t) = \sum_{k=0}^{\infty} x_k.e^{j(w_c.t+\theta_k)}$$

a_0 and s_0 being the amplitude of the direct and specular reflection, respectively; Φ and $\Phi^{'}$ their phase angle. The diffuse component is composed of a large number of incoherent components each having an amplitude $x_{\ k}$ and phase angle θ_k [1]. The corresponding expression of the in phase and quadrature component is:

$$R_i(t) = a_0.cos(\Phi) + s_0.cos(\Phi^{'}) + x_i(t)$$
$$R_q(t) = a_0 sin(\Phi) + s_0.sin(\Phi^{'}) + x_q(t)$$

The model assumes that the in phase and quadrature components of the diffuse component are independent zero-mean Gaussian variables having probability with zero mean and variance σ^2 (i.e. $x_i(t)$ ant $x_q(t)$ are $N(0,\sigma^2)$), that the distribution of Φ and Φ' are uniform (i. e. $p(\Phi) = 1/2\pi$).
The amplitude and the phase of the received signal is then:

$$\begin{aligned} \nu(t) &= \sqrt{R_i(t)^2 + R_q(t)^2} \\ \phi(t) &= tan^{-1}\frac{R_q(t)}{R_i(t)} \end{aligned}$$

From here we can calculate the probability density of the amplitude ν and from the phase ϕ.

If no specular reflection is present ($s_0 = 0$) and, if we assume, with no loss of generality, that $\Phi = 0$ the Rician distribution can be deduced

$$\begin{aligned} p[\nu] &= \frac{\nu}{\sigma^2}e^{-(\frac{\nu^2+a_0{}^2}{2.\sigma^2})}I_0(\frac{\nu a_0}{\sigma^2}) \\ p[\phi] &= \frac{1}{2\pi}e^{-\frac{C}{M}}[1+\sqrt{\pi\alpha}e^{\alpha}(1+\text{erf}(\sqrt{\alpha}))] \\ \text{with } \alpha &= \frac{C}{M}cos^2(\phi) \end{aligned}$$

where C/M is called the carrier to multipath ratio $\frac{C}{M} = \frac{a_0{}^2}{2\sigma^2}$.

The Rayleigh distribution is gained if in addition to the assumptions for Rice the direct path is blocked ($a_0 = 0$), then

$$\begin{aligned} p[\nu] &= \frac{\nu}{\sigma^2}e^{-\frac{\nu^2}{2\sigma^2}} \\ p[\phi] &= \frac{1}{2\pi}\ . \end{aligned}$$

The Rician distribution is often used to describe line-of-sight (LOS) case ("Good State"). The Rayleigh distribution is used for the non line-of-sight (nLOS) "Bad State" in case of blockage. A propagation experiment typically contains "good state" period (for instance open areas) and bad state period (for instance urban environment with a lot of surrounding buildings).

The frequency used for the forward and the return link are separated by approximately 200 MHz. Random effects, such as signal blockage, affecting the channel on the forward link are expected to be the same on the return link. Concerning correlation between forward and return link, the best case is when the forward link has the same behaviour as the return link. In this case, the difference between the return and the forward should be zero, and it is possible to predict return link behaviour from forward link measurement and vice-versa. If the forward and the return link are "uncorrelated" the difference should be random with zero mean because we expect that the multipath component will be uncorrelated between both links.

CAMPAIGN RESULTS

A typical example is shown in Fig. 2. In this example, two diverse uplink paths and two diverse downlink paths are measured simultaneously, as depicted in Fig. 2. The received power of path # 1 downlink (line 1),path # 2 downlink (line 2), path #1 uplink (line 3), and path #2 uplink (line 4) is given versus time. The environment under test was urban with several 3 or 4 storey buildings and a number of trees in the vicinity. The mobile terminal was a handheld and the user was walking in a random fashion for the duration of the test. Signal blockage by buildings and trees, and head blockage occurred during the test. These can be observed in the measurements. Good and bad channel states can be observed as well as specular reflection resulting in strong two-path fading (for instance line 3, time 45…55 sec). Furthermore, the benefit of satellite diversity can be seen in this particular urban environment where blockage of one transmission path coincides with visibility to the alternative satellite. This is an interesting, but somewhat special scenario and many others were observed where blockages to both paths coincided. In these cases, reliable, continuous communication would only be possible with link margins sufficient to penetrate such blockages or provide sufficiently strong reflected components. Since these link margins are not viable for power limited satellite based systems, diversity provides a limited, but best available option for some extension of coverage.

The available results enable us to analyse :

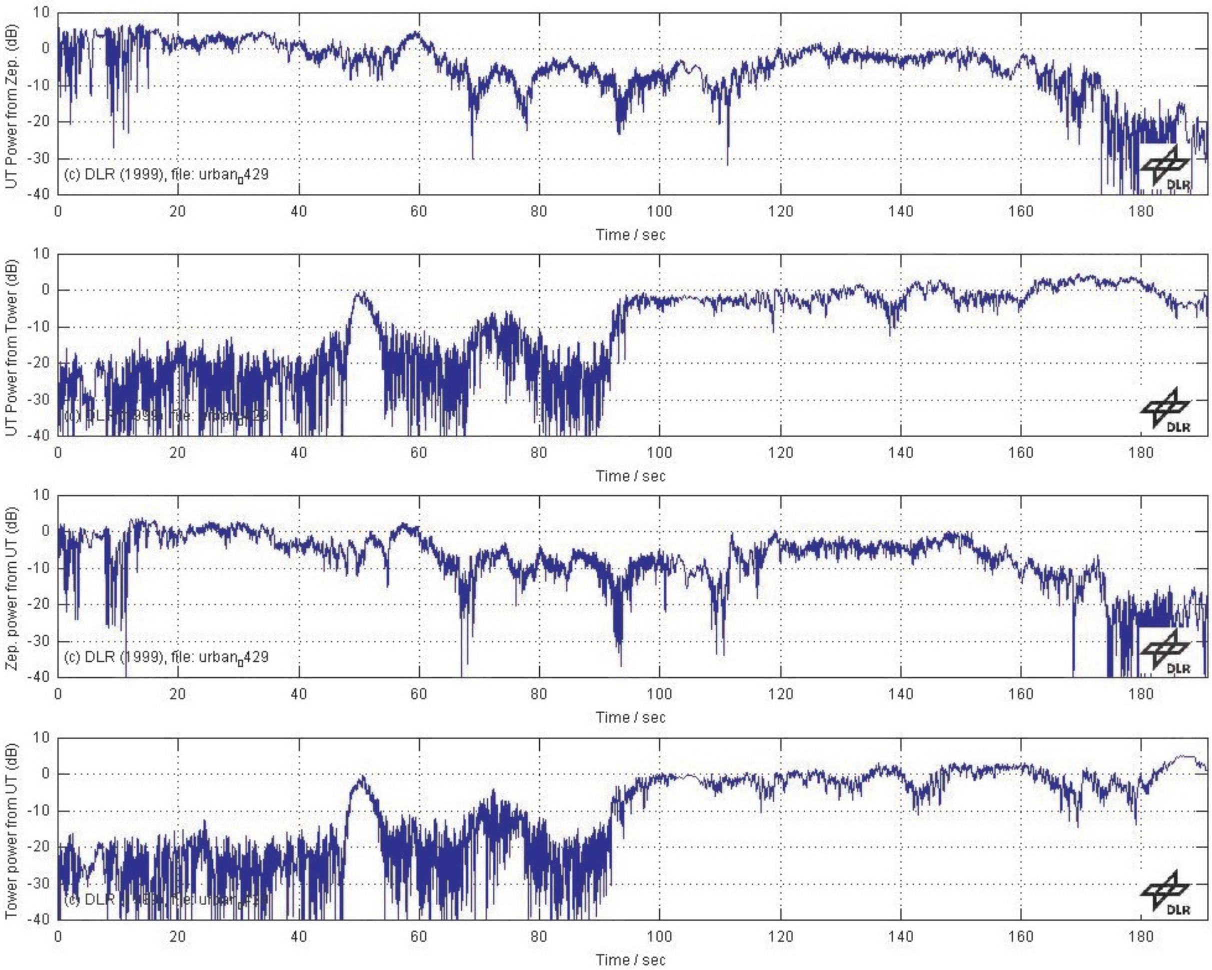

Figure 2: Exemplary measurement result, urban environment, satellite elevation 25 and 45 deg.

- the coverage of the future system in outdoor and indoor environment,
- the potential benefit of diversity for extended coverage,
- the correlation of forward and return link : these results will be presented in the next sections.

CHANNEL CORRELATION

Firstly, a subjective analysis of the time variation of the recieved signal on the different link has been conducted.

In many cases, strong de-correlation between forward and return link paths is apparent, caused by the difference in the transmission frequencies. Typically, the strongest de-correlation, where an increase in the signal in one direction corresponds to a decrease in the other direction, occurs on low signal levels.

Level dependency

When the level on the link is high (-10 dB / 0 dB), the behaviour is highly correlated. When the level on the link is between -20 and -10 dB, the behaviour is correlated but some effects (like fast fading) may occur only on one of the links. When the level is below this level the results are case-dependant. Sometimes the correlation still remains, other times the link has completely different behaviour in both directions. This result (level dependency of correlation) can be explained — assuming that the channel is Ricean — by a decrease of the C/M (carrier to multi-path ratio). The diffuse component remains the same and the signal amplitude decreases. We can use the model presented in the above section to describe the measurement. The direct path component is the same on both directions and the diffuse component different on both directions. If the C/M ratio is large, the channels are highly correlated and when it is small, the channels are not correlated.

Importance of differences

Good correlations do not imply no differences between the transmission directions. Signal plots clearly show that it is possible to have variances in the current level of both links. These variances can be explained by the diffuse component that is different in both directions. Effective power control algorithms should avoid responding to those fluctuations in current level, because both links have the same power level only on a long-term average, and instantaneous values can vary even when the correlation is good.

POWER CONTROL

Power control is often employed to minimise user equipment power requirements, and to minimise adjacent channel and co-channel interference effects. Generally power control functions can be performed in both the user equipment and the base station equipment. The radio propagation results from the measurement campaign have been used in a generic study of power control algorithms. Three main categories of power control were considered. The first one is called long-term power control and refers to the allocation of power at the satellite level, it assures the power management on the various spotbeams of the satellite. The second one is called medium-term power control. In this control, carrier levels are managed on a call-by-call and timeslot-by-timeslot basis. The third one is called short-term power control and it is done second-per-second, at the base station and at the user side in order to maintain a given E_b/N_0.

Long-term power control This concerns only the power management at the spacecraft. The spacecraft power management is under control of the satellite resource management unit. It needs to know the characteristics of the satellite transponder (how $P_{sat_{in}}$ is related to $P_{sat_{out}}$).

Medium-term power control This call-by-call control is done during the call initialisation to set-up the power allocated by the long term power control for an individual call. It sets-up some initial values that will be used by the short-term power control algorithm (initial transmit value, maximum allowed transmit value and a margin). This process guarantees a target E_b/N_0 at the user side.

Short-term power control This is done both at the base station and user side to counteract the variation of the power level in the satellite channel. The algorithm can be either an open loop algorithm or a closed loop power control. The open loop algorithm is quicker than the closed loop algorithm, but relies on using the measurement of one link to estimate the status of the other link (and is only effective against effects where there is strong forward and return link correlation, such as signal blockage). Example results of a simulation of the performance of this scheme are shown in Fig. 3. The upper graph shows a power series with a deep fade. The base station attenuation settings represent the actual value of the power control. During the fade, the power attenuation is decreased to compensate the fade. Due to the inherent measurement time the compensation has some delay, and a short increase in the BER (lower graph) is visible, however, the received voice packets (blocks above the BER line) can be still decoded correctly.

REFERENCES

[1] Lutz, E., Werner, M., and Jahn, A., *Satellite Systems for Personal and Broadband Communications*, Springer-Verlag, London, 2000.

[2] Ghedia, L., Smith, K., and Titzer, G., “Satellite PCN – the ICO system,” *International Journal of Satellite Communications*, Vol. 17, 1999, pp. 273–289.

[3] Lutz, E., Cygan, D., Dippold, M., Dolainsky, F., and Papke, W., “The Land Mobile Satellite Communication Channel — Recording, Statistics and Channel Model,” *IEEE Transactions on Vehicular Technology*, Vol. 40, 1991, pp. 375–386.

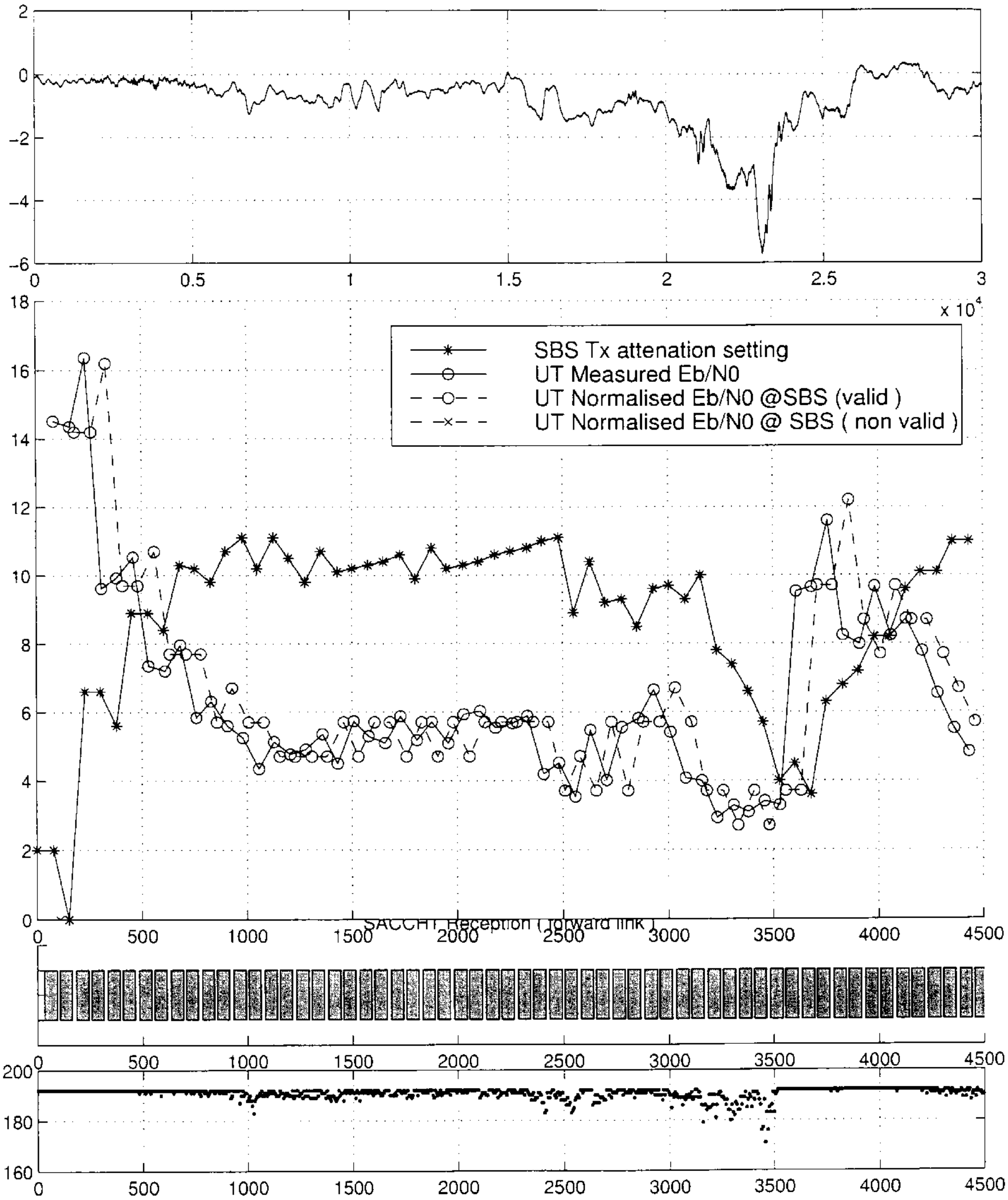

Figure 3: Exemplary simulation of a closed loop power control using measured data.